Photonics-assisted joint radar and communication system in W band using electromagnetic polarization multiplexing

Mingzheng Lei[1], Yuancheng Cai[1,2], Jiao Zhang[1,2], Bingchang Hua[1], Yucong Zou[1], Wei Luo[2], Miaomiao Fang[2], Shitong Xiang[2], Jianjun Yu[1,3], and Min Zhu[1,2,*]
[1]*Purple Mountain Laboratories, Nanjing 211111, China*
[2]*National Mobile Communications Research Laboratory, Southeast University, Nanjing 210096, China*
[3]*Key Laboratory for Information Science of Electromagnetic Waves, Fudan University, Shanghai 200433, China*
**minzhu@seu.edu.cn*

Abstract: We proposed and demonstrated a photonics-assisted joint radar and communication system in W band using electromagnetic polarization multiplexing. The spatial resolution and wireless rate have reached a record of 15 mm and 92 Gbit/s, respectively. © 2023 The Authors

1. Introduction

The coexistence of radar and communication in millimeter-wave (mmW) bands has urgently driven the integration of sensing and communication to simplify the hardware and software resources. Thanks to the inherent high frequency and large bandwidth enabled by photonics, photonics-assisted joint radar and communication (JRC) methods have drawn extensive attentions [1-9]. The mmW radar and communication functions can be realized in time-division multiplexing (TDM) [1-2], frequency-division multiplexing (FDM) [3-4], and co-time and co-frequency (CTCF) modes [5-9], respectively. Note that the CTCF mode not only avoids the interruption of sensing and communication in the TDM mode, but also avoids the mutual interference between radar and communication in the FDM mode. Unfortunately, due to the use of integrated waveforms, it is difficult for these CTCF-based JRC systems to achieve ultra-high spatial resolution and data rate simultaneously, as illustrated in Fig. 1.

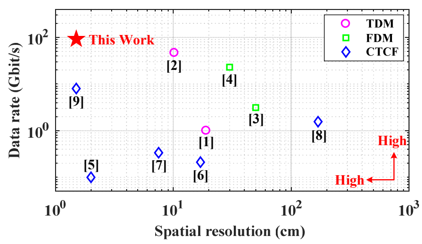

Fig. 1. Typical research works on photonics-assisted JRC system.

In this work, we have proposed a photonics-assisted CTCF-based JRC system in W band using electromagnetic polarization multiplexing. The up-conversion of the radar and communication signals to W band is implemented by combining the asymmetrical single-sideband (ASSB) with heterodyne detection. The radar and communication functions are assigned on two orthogonal electromagnetic polarizations, which makes full use of the time-frequency resources to obtain ultra-high spatial resolution and data rate at the same time. Experimental results show that the spatial resolution of up to 15 mm and data rate as high as 92 Gbit/s are realized simultaneously, which is superior to all the typical works on photonics-assisted JRC system [1-9] in terms of both spatial resolution and wireless rate.

2. System Description and Principle

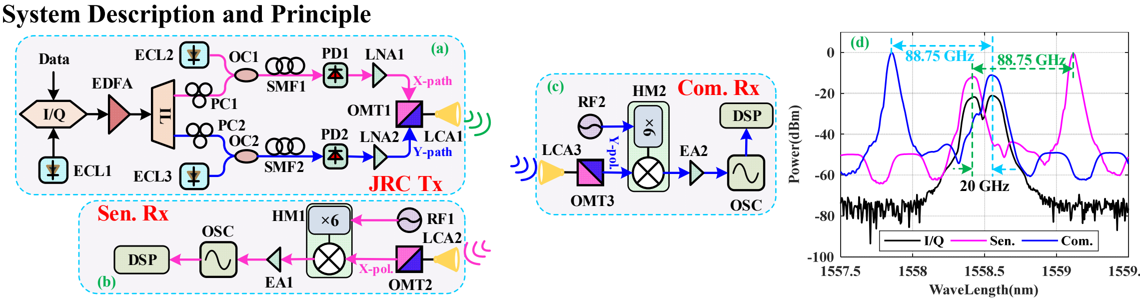

Fig. 2. Schematic diagram of (a) JRC Tx, (b) sensing Rx, and (c) communication Rx; (d) optical spectra at different nodes of the JRC Tx.

The proposed photonics-assisted JRC system consists of three parts, namely, the JRC transmitter (JRC Tx), the sensing receiver (Sen. Rx), and the communication receiver (Com. Rx), as shown in Figs. 2(a)-(c), respectively.

In the JRC Tx, a light wave (L1) from an external cavity laser (ECL1) is launched into an I/Q modulator. The two arms of the modulator are driven by the real and imaginary parts of a complex signal, respectively. The complex signal is a linear combination of the IF radar and communication signals located in opposite carrier frequencies. By appropriately biasing the modulator to implement ASSB modulation, two sidebands (i.e., Sen-OSB and Com-OSB) centered on the L1 can be obtained. After the power compensation for the modulation loss by an erbium-doped fiber amplifier (EDFA), an interleaver (IL) separates the two sidebands. The separated Sen-OSB is coupled with a local oscillation (LO1) from the ECL2 for sensing, while the separated Com-OSB is combined with the LO2 from the ECL3 for wireless communication. The sensing signal is transmitted over a single-mode fiber (SMF1) to a remote photodetector (PD1). Meanwhile, the communication signal is transmitted to the PD2 through the SMF2. By heterodyne beating of the sideband and respective LO, the mmW radar/communication signal in X-/Y-pol can be generated in the PD1/PD2. Notably, two polarization controllers (PCs) before the optical couplers (OCs) are used to maximize the mmW powers. The radar signal in X-path and the communication signal in Y-path are first boosted by two low noise amplifiers (LNAs), and then combined by a mmW orthomode transducer (OMT1) for polarization multiplexing. Thus, the radar and communication signals can operate in a CTCF mode, and radiated into free space via a lens corrected antenna (LCA1).

In the sensing Rx, the mmW signals reflected by the user are received by the LCA2 and polarization filtered by the OMT2. Thus, only the radar echo in X-pol will pass through the OMT2. The radar echo is then down-converted to the IF band by a harmonic mixer (HM1), which integrates a ×6 frequency multiplier chain and operates with a RF clock (RF1). The down-converted IF radar echo is further amplified by an electrical amplifier (EA1) and digitized by an oscilloscope (OSC) for offline digital signal processing (DSP).

In the communication Rx, the mmW signals are received by the LCA3 and polarization filtered by the OMT3. Instead, only the communication signal in Y-pol will pass through the OMT3. The downlink signal is then down-converted to the IF band by the HM2, which is driven by the RF2. The down-converted IF communication signal is further power compensated by the EA2 and digitized by an OSC for offline demodulation.

So far, a photonics-assisted mmW JRC system operated in a CTCF mode by using electromagnetic polarization multiplexing is structured. Because all time-frequency resources can be used for sensing and communication at the same time, the proposed novel JRC system can contribute to both the ultra-high spatial resolution and data rate.

3. Experimental set-up and results

A proof-of-concept set-up experiment is designed according to Figs. 2(a)-(c). The wavelengths of the L1, L2, and L3 are set at 1558.492 nm, 1559.122 nm, and 1557.862nm, respectively. The power of the L1 is fixed at 14.4 dBm, which is 4.4 dB higher than that of the L2 and L3, given the loss of the I/Q modulator. The combined IF radar and communication signals are generated by a 92-GSa/s arbitrary waveform generator (AWG) to drive the modulator. Initially, the IF radar signal is a linear frequency-modulated (LFM) wave with a carrier frequency of 10 GHz and a bandwidth of 11.5 GHz. The IF communication signal is a 11.5-GBaud 16QAM signal centered at 10 GHz. The modulator is automatically controlled to implement ASSB modulation. As a result, two sidebands spaced by 20 GHz can be observed at the output of the modulator, as shown by the black line in Fig. 2(d). The two sidebands are boosted to about 10 dBm by an EDFA and then separated by an IL. The lengths of the SMF for sensing and communication are 50 m and 100 m, respectively. After the SMF, the optical power in each path is attenuated to 4 dBm by two variable optical attenuators (VOAs). The measured optical spectra for sensing and communication are shown as the pink and blue lines in Fig. 2(d), respectively. From Fig. 2(d), the wavelength space between the LO1/LO2 and Sen-OSB/Com-OSB is calculated to be about 0.71 nm. Thus, the mmW LFM/16QAM signals centered at about 88.75 GHz will be generated in the PDs. The generated mmW signals are first boosted by about 35 dB, then polarization multiplexed by the OMT1, and finally radiated into the free space via the LCA1 with a gain of 30 dBi.

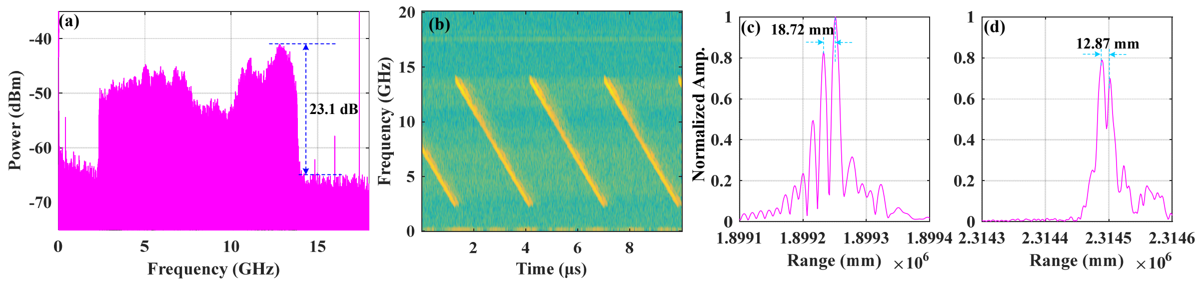

Fig. 3. (a) Electrical spectrum and (b) time-frequency characteristics of the down-converted echo; normalized cross-correlation between the down-converted echo and the reference LFM wave when the bandwidth is set at (c) 11.5 GHz and (d) 23 GHz.

For radar detection, two metal plates serving as two users are placed about 10.8 m away from the perpendicular bisector of the LCA1 and LCA2. The longitudinal distance between two users is 15.0 mm. The transverse distance between the two antennas is about 32 cm. Owing to the polarization isolation, basically only the mmW LFM echo passes through the OMT2. The passed echo is down-converted by a 96-GHz RF clock and then power compensated by the EA1 with a gain of 26 dB. Figure 3(a) shows the spectrum of the obtained echo signal, which is more than 23 dB higher than the noise floor. Figure 3(b) shows the time-frequency characteristics of the down-converted echo. The frequency varies periodically and linearly between about 2-14 GHz. Figure 3(c) show the normalized cross-correlation between the down-converted echo and its reference. The distance space between the two distinct peaks is 18.72 mm, which is close to the actual value of 15.0 mm. To test the bandwidth flexibility, the carrier frequency and bandwidth of the IF LFM wave are changed to 14 GHz and 23 GHz, respectively. The calculated normalized cross-correlation is shown in Fig. 3(d). The two distinct peaks have a spacing of 12.87 mm, leading to a ranging error less than 3 mm.

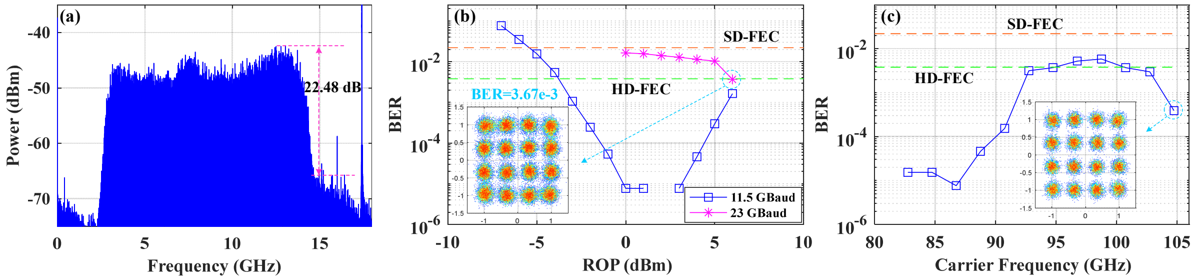

Fig. 4. (a) Electrical spectrum of the down-converted 16QAM signal; (b) calculated BER as a function of the ROP at 11.5 GBaud (blue) and 23 GBaud (pink); (c) calculated BER as a function of the mmW frequency at 11.5 GBaud.

For wireless communication, the LCA3 is 10.8 m away from the LCA1. Thanks to the polarization isolation, basically only the downlink mmW 16QAM signal passes through the OMT3. The passed communication signal is also down-converted by a 96-GHz clock and then power compensated by the EA2 with a gain of 26 dB. Figure 4(a) shows the spectrum of the down-converted 16QAM signal, which is more than 22 dB higher than the noise floor. Notably, the spectrum in Fig. 4(a) occupies almost the same frequency range as that in Fig. 3(a), indicating that the proposed JRC system successfully operates in a CTCF mode. To test the optical power margin of the downlink communion, we calculate the bit error rate (BER) under different received optical powers (ROPs). During the measurement, the optical power into each PD is equal for simulating the power distribution. The calculated BER as a function of the ROP is shown as the blue line in Fig. 4(b). The optimal optical power is about [0, 4] dBm. Furthermore, when the optical power is within [-2, 6] dBm, the calculated BER is better than the hard-decision forward-error-correction limit (HD-FEC, BER=3.8e-3). Also, the bandwidth flexibility is tested by switching the IF communication signal to a 23-GBaud 16QAM signal centered at 14 GHz. The BER versus the ROP is shown as the pink line in Fig. 4(b). At a 6-dB ROP, the communication performance with the BER of 3.67e-3 is slightly better than the HD-FEC, and its constellation diagram is inset in Fig. 4(b). The slightly divergent constellation points indicate that data rate of up to 92 Gbit/s is successfully achieved. Figure 4(c) shows the BER at different transmission frequencies. The communication performance of the 11.5-Gbaud 16QAM signal is better than the soft-decision forward-error-correction threshold (SD-FEC, BER=2.2e-2) within the whole W band. At a 104.75-GHz frequency, good communication performance can still be obtained, as shown in the inset of Fig. 4(c).

4. Conclusion

We have proposed and experimentally demonstrated a photonics-assisted JRC system in W band. The radar and communication functions are operated in a CTCF mode using electromagnetic polarization multiplexing. Therefore, all time-frequency resources can be simultaneously applied to the two functions, resulting in a spatial resolution of up to 1.5 cm and wireless rate as high as 92 Gbit/s. The proposed JRC system operating in the entire W band is expected to play an important role in the upcoming mmW era.

This work was supported jointly by the National Natural Science Foundation of China (62201393, 62201397); Natural Science Foundation of Jiangsu Province (BK20220210, BK20221194); and Open Fund of IPOC (BUPT, IPOC 2021A01).

References

[1] A. Kanno, et al., *IEEE IRMMW-THz*, pp. 1-2 (2015).
[2] Y. Wang, et al., *Opt. Lett.* **46**(24), 6103-6106 (2021).
[3] R. Song et al., *Opt. Lett.* **47**(11), 2931-2934 (2022).
[4] M. Lei, et al., doi: 10.1109/JLT.2022.3181608. (2022).
[5] H. Nie, et al., *IEEE MWP*, pp. 1-4 (2019).
[6] S. Wang, et al., *Appl. Opt.* **61**(16), 4752-4760 (2022).
[7] Z. Xue, et al., *Opt. Express* **29**(14), 22442-22454 (2021).
[8] L. Huang, et al., *JLT* **37**(21), 5406-5416 (2019).
[9] W. Bai, et al., *Opt. Express* **30**(15), 26407-26425 (2022).